Estimating Core Body Temperature Using Electrocardiogram Signals

Chie Kurosaka (chie-k@health.uoeh-u.ac.jp)
University of Occupational and Environmental Health
Takashi Maruyama
University of Occupational and Environmental Health
Shimpei Yamada
University of Occupational and Environmental Health
Yuriko Hachiya
University of Occupational and Environmental Health
Yoichi Ueta
University of Occupational and Environmental Health
Toshiaki Higashi
Industrial Health Consultant Nishinihon Occupational Health Service Center

Research Article

Keywords: core body temperature, estimated model, heatstroke, electrocardiogram

Posted Date: April 30th, 2021

DOI: https://doi.org/10.21203/rs.3.rs-469706/v1

Abstract

Purpose: Core body temperature is one of the diagnostic criteria for heatstroke. This study proposed an algorithm that estimates core body temperature based on electrocardiogram signals that are received by a wearable sensor.

Methods: A total of 12 healthy males aged 21–64 years performed an ergometric exercise load test in an environmental chamber adjusted to a temperature of 35°C and humidity of 50% under two exercise conditions. Physical data were obtained from participants pre- and post-experiment, while electrocardiograms, core body temperatures, and body surface temperatures were continuously measured. Amount of change in core body temperature was estimated by multiple regression analysis wherein indexes derived from electrocardiograms was treated as the dependent variables.

Results: Findings showed that continuous core body temperature can be estimated using electrocardiogram signals regardless of individual characteristics such as age and physique.

Conclusions: In this study, we developed a core body temperature estimation model using the Poincaré plot method. Changes in heartrate were related to heat production and yielded valid results. As the basic estimation model is positioned for use under limited conditions, we also plan to enhance estimation accuracy and further verify efficacy in consideration of clothing and environmental conditions.

1. Introduction

Heatstroke has become a more prevalent occurrence in recent years, thus constituting a social problem. In this regard, countermeasures include changes to outdoor working conditions, altered working hours in business and educational settings, environmental improvements designed to facilitate break times, and educational provisions concerning the nature of the issue itself. More specifically, heatstroke is a disease in which the body reaches an imbalance in salt-water content while operating in a hot environment, thereby resulting in a failure of the body's temperature regulation function. As severe cases of heatstroke can be life-threatening, it is important to ensure proper occupational health management (e.g., water supplementation and rest) in addition to providing health education aimed at raising awareness about appropriate preventive measures. While these elements have proactively been implemented in a variety of contexts, deaths continue to occur as a result of heatstroke. To complicate matters, the Intergovernmental Panel on Climate Change (IPCC) [1] issued a report showing substantial rises in global average surface temperatures over the past 50 years due to global warming, which has largely been triggered by human activity. As this is a worldwide issue, international efforts are targeted at reducing greenhouse gas (GHG) emissions, starting with CO_2. However, these improvements will take time, in which case temperatures are continually expected to rise over the foreseeable future. This makes it urgent to develop and implement technologies that can continuously manage changes in physical condition during activity in hot environments.

When evaluating heat stress, it is important to consider factors related to heat dissipation from the human body (e.g., radiative heat (radiation temperature) and wind speed) in addition to measurable environmental factors (e.g., temperature and humidity). These risk factors must be comprehensively evaluated even in relatively cool environments, as the heat transfer rate varies due to exercise intensity and several other items of concern, including the heat retention/thermal insulation properties of clothing, age, and physical condition. The wet-bulb global temperature (WBGT) index is widely known to meet these requirements with a high degree of convenience and reliability; it has thus been adopted by international organizations such as the American Conference of Governmental Industrial Hygienists (ACGIH) [2] and International Organization for Standardization (ISO) [3]. The WBGT index is calculated based on the natural wet-bulb temperature, black-bulb temperature, and air temperature. ISO7243 [3] recommends that any countermeasures aimed at heatstroke onset risk should be performed according to both heat acclimation and airflow; here, the allowable heat standard value is classified into 14 categories based on work intensity.

In addition, the International Organization for Standardization issued four heat risk evaluation indexes for determining work discontinuation under ISO9886, including core body temperature (rectal temperature, esophageal temperature, intraperitoneal temperature, tympanic membrane temperature, ear canal temperature, urine temperature), skin temperature (local site, multiple site average), heart rate, and body weight reduction [4]; a rectal temperature of 38.0–38.5°C and skin temperature of 43°C (according to heat acclimation) are given as work stoppage threshold values. ISO9886 also states that the maximum heart rate should not exceed a threshold of 185 − 0.65×(age) or continuous heart rate 180−(age). Moreover, ACGIH guidelines recommend the termination of heat exposure in cases where the heart rate does not return to 120 or less within one minute after reaching peak work intensity.

Body temperature is roughly categorized into brain/internal organ temperature (core body temperature) and skin surface temperature. Because elevated core body temperature increases the risk of heatstroke onset, it is desirable to measure this at a location that is as close to the inside of the body as possible (e.g., the tympanic membrane or rectum). At present, however, there is no easy method of measuring core body temperature continuously and non-invasively during work, although several studies have proposed the idea of simulating changes in the human body temperature by modeling its heat production and dissipation mechanisms [5][6]. These models separate the body into several nodes, then formulate biomarkers that are correlated with body-temperature regulating mechanisms (e.g., perspiration, blood flow volume), heat transfer and production at various nodes, and heat dissipation to the outside. In this context, estimation precision is proportional to the number of nodes and calculation volume, which results in a mutually exclusive relationship. To accurately estimate body temperature during exercise, it is also important to use estimation methods that are based on temporally variable data. Among these methods, some studies have attempted to use recently developed devices that are designed to sense biodata (e.g., heart rate and body movement) when evaluating physical conditions in hot environments, thus providing a way to predict the risk of heatstroke [7][8]. Results have also suggested the feasibility of real-time heat stress evaluations that combine IoT technology and wearables. In biometric research, reliability increases when multiple indexes are combined; in terms of practicality, however, it best to avoid attaching a large number of sensors to the body, especially when methods are invasive. While devices must be wearable, they must also be designed

so they do not substantially restrict movement. Further, calculations should be both simple and focused on physiological indexes. For these reasons, electrocardiogram (ECG) signals are seen as a useful index for evaluating heatstroke risk, especially since calculations are simple. Because non-linear analyses and frequency analyses of the R-R interval (RRI) obtained from ECG signals have become widely used and well-known as typical indexes of autonomic nervous system activity [9][10][11][12], we believe it would be useful to estimate the risk of heatstroke based on the decomposition of ECG signals into biomarkers showing various relevant characteristics. As core body temperature is used as a diagnostic criterion for heatstroke, this study proposed and assessed the efficacy of an algorithm designed to estimate core body temperature based on ECG signals.

2. Methods

2.1. Participants

For the experiment, participants included a total of 12 healthy males aged 21–64 years (mean age ± SD = 39.6 ± 13.4) (Table 1). We preliminarily confirmed that they were free of arrhythmia and any diseases related to the cardiovascular system. None were taking medications. After receiving written descriptions of the experiment, all participants completed informed consent forms. Further, each observed regulated diets beginning with dinner on the previous day and lasting through breakfast on the test day (alcohol consumption was prohibited). Participants were also instructed not to consume caffeine on the day of the experiment. Further, they were told to unify their sleeping environments; this included a bedtime of 23:00 on the day prior and wake time of 6:00 on the day of the experiment. All participants provided written informed consent. This study was received approval to conduct the experiment from the Institutional Review Board of the University of Occupational and Environmental Health (Approval No. H29-213). The experiment was done in accordance with relevant guidelines and regulations.

Table 1
Participants and environmental conditions

No	Participants	Age	Height (cm)	Weight (kg)	Conditions	Exercise Load	Status	Note
1	S01	57	169	62	A	80W	Discontinued	Poor physical condition, data loss
2	S02	47	175	103	A	80W	Completed	
3	S03	46	170	57	A	80W	Discontinued	Rectal temperature reached 38.5°C
4	S04	64	174	70	A	80W	Discontinued	Poor physical condition
5	S05	53	167	66	A	80W	Completed	
6	S07	26	184	90	A	80W	Completed	
7	S06	31	173	85	A	80W	Completed	Data loss
8					B	120W	Discontinued	Poor physical condition
9	S08	21	175	61	A	80W	Completed	
10					B	94W	Completed	
11	S09	27	172	80	A	80W	Completed	
12					B	157W	Completed	
13	S10	31	165	67	A	80W	Completed	
14					B	104W	Completed	
15	S11	28	167	64	A	80W	Completed	
16					B	109W	Completed	
17	S12	44	184	93	A	80W	Completed	
18					B	114W	Completed	

Notes: In test runs with different exercise intensities, six subjects participated in conditions A and B; thus, there were 18 total test runs. Of these, three cases discontinued measurements because the discontinuation criteria were met, while two cases were excluded from analysis due to data loss.

2.2. Experiment Procedure

The exercise load test was performed in an environmental chamber adjusted to a temperature of 35°C and humidity of 50% (WBGT approximately 30°C). The experiment was performed in the following order: rest for six min; exercise load, 18 min; rest for 18 min; exercise load, 24 min; rest for 18 min. Physiological signals were measured continuously while the rate of perceived exertion (RPE) was assessed every three minutes from the start of the experiment. A board on which the score was written was placed in front of the test subjects, and RPE was recorded after having the subjects point to the location in question. The experiment was immediately discontinued when the experiment discontinuation criteria were met (core body temperature exceeding 38.5°C, convulsions, headache, dizziness, nausea/vomiting, blank expression, loss of consciousness, elevated levels of RPE). A Health Guard II ergometer was used during the test (Takei Scientific Instruments Co., Ltd.). As for the exercise loads, the ergometer was set to an intensity of 80 W for Condition A; maximum oxygen intake was measured beforehand at 60% for Condition B (where VO_2 = 3.5 + 3.5+(1.8×Work rate) ÷ Body weight, and 1 W = 6.12× Work [kg□m/min] [13]. As six of the participants who engaged in Condition A performed Condition B on a different day, a total of 18 test runs were conducted.

2.3. Physiological Measurement

Both pre- and post-experiment, participants were measured for body weight using a precision scale (Combics 1 plus, Sartorius); they were also measured for fat percentage, fat-free mass, muscle mass, body water content percentage, and basal metabolic rate using a multi-frequency segmental body composition analyzer (MC-780A, TANITA). During the experiment, we continuously measured ECG, core body temperature (rectal temperature), and body surface temperature (chest, palms, outer surface of sensor, inner surface of sensor). The ECG was recorded at a 1.5kHz sampling interval with a BSM-2401 wireless electrocardiograph (Nihon Kohden Corporation), while both core body temperature and body surface temperature were measured with a thermocouple and recorded via computer at 10-second intervals. We also collected the RPE every three minutes as a measure of subjective exercise intensity.

2.4. Analysis Methods

Regarding precise body weight measurement data, we analyzed differences due to exercise loads through a repeated t-test of the changes. We also calculated differences before and after (Δ = after-before) for each physical data item and investigated the relationship between muscle mass and height (relative muscle mass). Regarding the analysis test runs in which both conditions participated (n = 5), we examined the differences between conditions using a signed test.

Regarding physiological responses, we analyzed 16 total cases, but two were excluded for lacking measurement data (Table 1; No. 1, No. 6-A). The continuous measurement data were divided into 28 three-minute blocks (Rest1-1 – Rest1-2, Ergo1-1 – Ergo1-6, Rest2-1 – Rest2-6, Ergo2-1 – Ergo2-8, and Rest3-1 – Rest3-6); we also examined correlations between various physiological data. Test runs in which the experiment was discontinued were subjected to analysis up to the block at which a three-minute period could be assured. We extracted the RRI from the ECG, then conducted a Poincaré plot analysis and HRV frequency analysis in each block; we calculated six indexes, including average RRI, SD1, SD2, LF, HF, and LF/HF. However, the frequency analysis was performed every six seconds to ensure a sufficient number of datapoints. For each plot, we derived the core body temperature and average amount of change in the core

body temperature Δtemp = temp(i + 1)-temp(i). We also examined the correlations between the six indexes. In this regard, we derived the Euclidean distance of each physiological index as converted into a standard score for each subject and examined the degree of similarity in the time series data for both core body temperature and the ECG signals. As such, we extracted parameters that should be useful for estimating core body temperature; this index was examined by combining the time series data with mathematical findings, in which we calculated 11 dependent variables (e.g., relative amount of change). Of those, we deleted variables for which the multi-covariate index VIF was 10 or greater, then conducted a multiple regression analysis (forced entry method) wherein the amount of change in core body temperature was treated as the objective variable (the IBM SPSS Statistics 19 software was used for analysis). Finally, we calculated the difference between the estimated value obtained in the estimation model and the actual measured value, thus confirming the model's validity.

3. Results

3.1. Experiment Implementation and Changes in Physical Data

Of the 18 total test runs, four were discontinued (i.e., three participants discontinued, of which, two due to poor physical conditions and one due to elevated rectal temperature; those who discontinued due to poor physical condition were the oldest participants in the study). For test runs in which both conditions were performed, the exercise loads were greater in Condition B. Table 2 presents a comparison of the physical data, including precision weight measurements before and after the comparison. As shown, weights and fat percentages were significantly reduced ($p < .001$, rate of change = 1.5%), while body water content percentages increased significantly ($p < .001$, rate of change = 3.03%). The ACGIH treats a 1.5% body weight reduction (before and after work comparison) as the heat exposure limit value [2]. The rate of weight change found in this study's experiment was extremely close to this threshold; thus, we were able to determine that environmental conditions associated with a high risk of heatstroke can be properly set. No relationship was observed between the differences (Δ = after-before) in each physical datum and relative muscle mass (r=-0.340 ~ 0.332), thus clarifying that such changes were not merely determined based on participant physique. In addition, no relationship was observed in either the body weight change or changes in the indexes thereof; regarding the test runs conducted under both conditions (n-5), body weight showed a greater reduction tendency in Condition B (mean ± SEM = -0.50 ± 0.14, $p = 0.063$, sign test). We observed no differences between conditions for other physical responses.

Table 2
Before and after comparison by precise weight measurement (Mean ± SEM)

	Before	After	p value		Change Percentage (%)
Weight (kg)	75.14 ± 3.57	74.04 ± 3.55	< .001	***	-1.50
Fat Percentage (%)	13.73 ± 1.83	12.63 ± 1.88	.001	**	-12.38
Fat-Free Mass (kg)	61.41 ± 2.12	61.43 ± 2.04	.946		-0.10
Muscle Mass (kg)	58.24 ± 2.01	58.25 ± 1.94	.962		-0.11
Body Water Content (%)	42.61 ± 1.46	43.94 ± 1.62	< .001	***	-3.03
Basal Metabolic Rate (kcal/day)	1743.38 ± 67.29	1738.31 ± 65.14	.550		-0.21

Note: Weight and fat percentage were significantly reduced, while the body water content percentage rose significantly in conjunction. The weight change was consistent with the weight loss rate of 1.5% proposed by the ACGIH; appropriate environmental conditions should be set due to the risk of developing heatstroke.

3.2. Time Series Changes in Physiological Responses

Figure 1(a) shows the time series changes in core body temperature, while Fig. 1(b) shows changes in the Δtemp of the core body temperature. Here, the core body temperature rose rapidly due to exercise loads, and did not substantially decline during the subsequent 18-minute rest period. In particular, a gentle rise continued during the first half of the rest period following the first exercise load (Rest 2); body temperature rose the same degree during the second exercise load as seen at the conclusion of the first exercise load. Approximately the same rises in core body temperature were observed due to the first and second exercise loads. Figure 1(b) and Fig. 2(a-d) show the time series data of the physiological indexes calculated from the ECG signals. Although the RRI average dropped rapidly due to exercise loads and rose during rest, the RRI during rest showed a shortening trend over time without returning to the pre-exercise state at 18-minutes of rest (Fig. 2(a)). The same trend for RRI was also observed in the Poincaré plot index. SD2 lengthened in blocks with status changes during rest periods following exercise loads, thus suggesting its possible usefulness in detecting postural and behavioral transformations (Fig. 2(b)). Regarding the HRV indexes for frequency analysis, both the LF and HF components disappeared during exercise loads. Further, it was difficult to ascertain the state during exercise loads within these frequency bands.

In the relationship between core body temperature and various physiological indexes, the results of the Euclidean distance measurements (Table 3) clarified changes in Δtemp with a higher degree of time series data similarity (i.e., rather than the core body temperature itself). When attempting to estimate core body temperature using ECG signals, these results show the efficacy of setting the amount of change in core body temperature as the objective variable, with the RRI average and Poincaré plot index set as the dependent variables.

Table 3
Euclidean distance of Core Body Temperature with Indexes from ECG signals

	Temp	Δtemp
RRI	8.52	4.88
SD1	8.46	5.65
SD2	7.96	5.49
LF	5.57	3.78
HF	5.81	3.90
LF/HF	4.45	4.56

Note: The time series data for each physiological index showed shorter Euclidean distances for the Δcore body temperature than core body temperature; a high degree of similarity was exhibited by the Δcore body temperature.

3.3. Multiple Regression Analysis

We observed the characteristics of the RRI average and Poincaré plot index, which are believed to be useful in estimating core body temperature; we treated 11 variables (RRI_{mean}, SD, SD1, SD2, $SD1_{low}$, $SD2_{low}$, $SD1_{up}$, $SD2_{up}$, SD(i)/SD(i-1), SD1(i)/SD1(i-1), and SD2(i)/SD2(i-1)) as candidate dependent variables. Poincaré plot indexes were defined by both the standard deviation vertical (SD1) and horizontal (SD2) to the identity line (SD1). Here, $SD1_{low}$ is the lower (origin point) SD1 bifurcated by the diagonal (y = x) in the Poincaré plot coordinates, while $SD1_{up}$ is the length of the top side. $SD2_{low}$ and $SD2_{up}$ are the values at the coordinates shifted by 90° (Fig. 3, Equations (1) and (2)).

$$SD_1^2 = \frac{1}{n}(\sum v_{di}^2 + \sum v_{ai}^2) \quad (1)$$

$$SD_2^2 = \frac{1}{n}(\sum h_{di}^2 + \sum h_{ai}^2) \quad (2)$$

By calculating the multiple covariate index VIF and eliminating variables for which VIF was 10 or more, we performed a multi-regression analysis of these variables using the forced insertion method, in which we treated the change volume of core body temperature (Δtemp) as the objective variable. As shown in Table 4, results suggested that the amount of change in core body temperature $\Delta Temp_{(i)}$ may be predicted by the functions $SD2_{(i)}$, $SD2_{(i-1)}$, and $\Delta Temp_{(i-1)}$ (Equations (3) and (4)). The degree of freedom adjusted decision coefficient of the estimation formula was 0.460 ($p < .001$).

$$\Delta Temp(j) = f(SD_2(j), SD_2(j-1), \hat{T}emp(j-1)). \quad (3)$$

$$\hat{T}emp(j) = Temp(0) + \sum_{i=1}^{j} \Delta Temp(i) \quad (4)$$

Table 4
Multiple regression analysis results

	Coefficient of regression	Standard error	*t*-value	*p*-value
Intercept	0.953	0.134	7.13	< .001
SD2	-0.078	0.004	-19.37	< .001
ΔSD2	0.005	0.001	6.60	< .001
^Temp	-0.022	0.004	-6.22	< .001

Note: The amount of change in core body temperature is shown in the SD2, ΔSD2, and previously estimated core body temperature; the degree of the freedom-adjusted decision coefficient was R2 = 0.460 (p < .001).

Figure 4 shows the averages for all test runs, including both the actual measurements and estimates of core body temperature. The mean error was − 0.007°C, while the mean error rate was − 0.02%. The maximum error was = 0.457°C in the test run in which the estimated value was largest when compared to the actual measured value (Supplement Fig. 1(a)), while the maximum error was = -0.445°C. in the test run in which it was smallest (Supplement Fig. 1(j))

4. Discussion

In this study, we developed a core body temperature estimation formula using ECG signals rather than individual characteristics such as age. Within the heat strain decision aid (HSDA) core body temperature prediction model, environmental conditions, clothing, and metabolic heat production were three important elements that were mutually attributable to core body temperature; for each participant, rises in core body temperature resulting from exercise were estimated based on individual characteristics, clothing, the environment, and activity status. Notably, the HSDA is also used for training purposes in the US military, and is currently being improved through multiple studies; specifically, it is being applied to predict safe work continuation times, suitable rest/water intake times, and even the risk of heatstroke, thus providing a preventive measure against it [14]. The model used in this study considered 16 dependent variables, with height being the primary variable among them (e.g., ambient temperature, clothing characteristics, environmental variables, such as humidity and temperature, physical activity, and dehydration).

Constantly fluctuating data, such as those pertaining to physical activity volumes are ideally collected in real time using wearable devices, which are suitable for daily use and do not greatly restrict movement. As such, some companies have implemented laborer health-management programs by monitoring biodata with wearable sensors that use IoT technologies; this promotes preventive behavior, which is initiated based on real-time warnings in cases where physical conditions are poor and/or the risk of heatstroke is increased. As discussed by Lin et al. [15], however, it is unlikely that verification and proof-of-concept experiments based on physiological characteristics are sufficient for proving the efficacy of these types of systems. While biometric information is easy to obtain using wearable devices, there are also several

limitations in terms of the required resources (e.g., power consumption, calculation power, and memory capacity) and communication status, which cannot always be ensured. In addition, power is needed to accomplish the so-called “synchronous” real-time processing, which simultaneously measures multiple biomarkers. Hence, it is important to study estimations that use as few biometrics as possible. From a practical standpoint, the estimation model used in this study is advantageous due to the employment of initial core body temperature values and ECG signals without the need for information pertaining to individual characteristics (e.g., the environment or clothing). In hot environments, the first physical response to heat exposure is dermal vasodilation, which dissipates heat outside the body by increasing the heat transfer rate of the body’s surface through an increase in dermal blood flow. Although this biological response is an efficient and effective response in mildly hot environments, excessive external heat is applied to the body under harsher temperature conditions, thus hindering the heat dissipation function. The blood also tends to accumulate in the extremities due to vasodilation, which causes a drop in both blood pressure and cerebral blood flow, the latter of which may result in dizziness, nausea, and fainting. As such, the body maintains its blood pressure by increasing its heart rate and cardiac output. In other words, heart rate is closely related to the thermoregulatory mechanism. From a physiological point of view, it is reasonable to use SD2 as an index for estimating the deep body temperature model because it shows a significant time-series change in heart rate. If system efficacy is ensured through this proposal, then it may be proactively used in high-risk workplaces as an effective countermeasure against heatstroke. Further, the use of various biometric sensors can not only prevent major health disorders resulting from heatstroke, but should also facilitate a wide range of other precautionary and health measures, including the prevention of industrial accidents due to lowered concentration and increased mental stress, daily health management, and elder care support.

The Poincaré plot analysis can calculate the nonlinear analysis indexes SD, SD1, and SD2 through a scatter diagram of the adjoining RRI intervals. The area of the ellipse valued at the SD (total HRV) correlates with baroreflex sensitivity (BRS), LF, HF, and RMSSD. The standard deviation in the short axial direction of the ellipse is referred to as SD1. This index demonstrates the short-term HRV of the rapid RRI change and is the same as the RMSSD [16]. SD1 is related to the coronary vagus nerve function. Reports have shown that it may be used to indicate exercise intensity (endurance drop) [17]. In contrast, SD2 demonstrates long-term HRV and is considered to be correlated with LF and BRS [18]. In this study, the RRI fluctuation was extreme, as it was used as verification in the exercise load test; compared to the amount of change in SD1, the SD2 index more noticeably captured RRI fluctuations. However, SD1 is still meaningful in cases where there is little overall change in RRI (e.g., desk work or light labor) or if the heart rate recovers in a short period of time. Although reports have shown that the ratio of SD1 to SD2 is useful as an index of sympathetic nerve activity [12], both indexes should be assessed based on physiological findings.

Both the HRV index used in the frequency analysis and that according to the RRI frequency analysis were composed of an LF component (low frequency component 0.04–0.15 Hz band) and an HF component (high frequency component 0.15–0.4 Hz band); it is thought that the LF component is mainly composed of Mayer wave-related sinus arrhythmia, which is derived from blood pressure, while the HF component is composed of respiratory sinus arrhythmia, which is derived from respiratory activity. The HF component

decreases in conjunction with the inhibition of parasympathetic nerve activity due to autonomic nerve disturbances and mental load. In this context, the LF/HF ratio to the LF component is considered to be an index of sympathetic nerve activity [9][19]. Castrillón et al. [20] have examined this index as an indicator of post-exercise recovery. It is important to note that most of the previous studies on this index have been validated by physiological measurements taken during desk work or in the context of standing up from the supine position, not during exercise, as in this study [19][21]. There also exist some negative findings regarding this index [22], so there is room for debate about the measurement conditions and other issues. Although these indexes capture gentle fluctuations between 0.04–0.4 Hz, they are not useful for the real-time detection of status during exercise loads. In this study, we were able to verify that both the LF and HF components disappeared during exercise loads; during those in which RRI becomes noticeably short with rapid respiration, we also believe that heart rate fluctuations shift to components other than the frequency bands thereby defined. While the well-known HRV index according to frequency analysis is now popular in simple stress measurement applications, it is crucial to ensure proper handling based on appropriate mathematical/physiological findings.

Regarding the estimation model proposed in this study, it is necessary to avoid actual measurements that tend to be higher than estimated values when targeting heatstroke prevention. Although the allowable range for the core body temperature estimation error is difficult to determine, a limit on the order of 0.5°C is probable if the properties of core body temperature are considered. Focusing on S09-B (Supplementary Fig. 1(j)), wherein the lowest core body temperature was estimated relative to the actual measurement, the participant in question was a very strong athlete, with an exercise intensity of 157 W (on par with hard labor) and maximum oxygen intake of 60%; this participant was obviously accustomed to exercise, as was also indicated through the interview survey. During exercise, the heart rate rises to supply oxygen to the body; however, physical training increases cardiopulmonary function, thus allowing the same exercise to be performed at a lower heart rate. In addition, as post-exercise heart-rate recovery (HRR) is correlated with the physical activity Baecke score, HRR is reportedly a useful index for exercise habits [23]. Although a previous study among athletes found a correlation between post-one-minute HRR and age [24], it is possible to use a post-three-minute recovery index to evaluate exercise adaptability. Considering daily exercise habits, S09 appears to have experienced a different heart rate variation and recovery trend than other participants; his Poincaré plot index also exhibited markedly gentle RRI changes. As such, the difference in this heart rate response trend is thought to have caused the estimation error.

This study also had some limitations. For one, the proposed estimation model was targeted at core body temperature increases during exercise loads in hot environments (35°C, 50%), in which case various environmental conditions remain unverified. Caution should therefore be taken when interpreting the results. Two, participants wore shorts when biometrics were assessed during the experiment. However, previous investigations using the HSDA model have implemented five types of protective clothing when engaging in treadmill exercises [25]. As the use of clothing substantially increases core body temperature, future studies should therefore verify the proposed model under different conditions (e.g., different clothing types and room temperatures).

Regarding ECG signals, there are many other indexes apart from those investigated in this study [26], including those that demonstrate vagus nerve activity in time regions such as pNN50 [27] and the regularity (complexity) of time-series data (e.g., approximate entropy and sample entropy) via nonlinear analysis [28] [29][30]. Although these indexes do not necessarily capture all the different types of phenomena, it is still possible to identify relationships and differences by contemplating indexes from a mathematical perspective. In other words, it is possible to achieve highly accurate estimation results through a diversified approach that decomposes the same biodata into multiple indexes, which may then be compared based on their unique differences and characteristics. Of course, it is also possible to add other physiological responses to phenomena that cannot be captured by ECG signals. Thus, this study should be considered an initial step, in which case we plan to conduct additional examinations.

5. Conclusions

This study demonstrated the efficacy of using ECG signals to estimate rises (amounts of change) in core body temperature during exercise loads in hot environments. In this context, the employed estimation model is characterized by its ability to continuously estimate core body temperature using both its initial value and ECG signals without the need for inputs related to individual characteristics (e.g., age and physique). However, there were also test runs in which the estimation error substantially increased, meaning that future investigations should address physical condition prior to engagement in exercise loads (constituting the initial value) and consider preexisting exercise habits among participants. Further, it is important to note that the proposed estimation model is designed for basic use under limited conditions. As such, we plan to improve the model for expanded usage (e.g., analyses of cases in which the core body temperature drops). In future studies, we also intend to consider the effects of different clothing types and exercise loads, thus demonstrating efficacy across a wider range of applications.

Declarations

Acknowledgements:

We express our heartfelt thanks to Mr. Monji and Ms. Nakase of the University of Occupational and Environmental Health environmental chamber for providing a study setting and experimental equipment. We also thank our research assistants, Ms. Okamoto and Ms. Uriu, who prepared the experiment and cooperated in recording and organizing the data.

Author contributions:

T.M. oversaw the research project. T.M., C.K., S.Y. and Y.H. designed the research plan and performed the experiment and data collection. C.K. and T.M. analyzed the data and wrote the manuscript. All authors reviewed the manuscript.

Competing interests:

This study was funded by Mitsufuji Corporation and Maeda Corporation under a joint research contract (PI: Takashi Maruyama).

Dr. Kurosaka is currently applying for the following patent.

Patent applicant (whether author or institution): institution

Name of inventors: Chie Kurosaka, Hiroto Sakamoto（Maeda Corp.）, Takeshi Matsumoto（Mitsufuji Corp.）

Application number: PCT/JP2020/034305

Status of application: Patent pending

Specific aspect of manuscript covered in patent application: The core body temperature estimating model is provided.

No other author has conflict of interest to declare relevant to this article.

References

1. IPCC. *Climate change 2013: the physical science basis. Contribution of working group I to the fifth assessment report of the intergovernmental panel on climate change* (ed. Stocker, T. F. & Qin, D. *et al.*) (Cambridge University Press, Cambridge, United Kingdom and New York, NY, USA, 2013).
2. ACGIH. TLVs and BEIs, heat stress and strain in *Threshold limit values for chemical substances and physical agents & biological exposure indices* (ed. ACGIH) 239-248 (ACGIH, 2019).
3. ISO7243. Ergonomics of the thermal environment — assessment of heat stress using the WBGT (Wet Bulb Globe Temperature) index. 2017.
4. ISO9886. Ergonomics — evaluation of thermal strain by physiological measurements. 2004.
5. Gagge, A. P., Stolwijk, J. A. J. & Nishi, Y. An effective temperature scale based on a simple model of human physiological regulatory response. *ASHRAE Trans.* **77**(2192), 247-262 (1971).
6. Stolwijk, J. A. A mathematical model of physiological temperature regulation in man in *NASA-Langley.* (National Aeronautics and Space Administration. Washington D.C. USA. NASA CR-1855, 1971).
7. Runkle, J. D. *et al.* Evaluation of wearable sensors for physiologic monitoring of individually experienced temperatures in outdoor workers in southeastern U.S. *Environ. Int.* **129**, 229-238 (2019).
8. Buller, M. J., Welles, A. P. & Friedl, K. E. Wearable physiological monitoring for human thermal-work strain optimization. *J. Appl. Physiol.* **124**, 432-441 (2018).
9. Task Force of The European Society of Cardiology and The North American Society of Pacing and Electrocardiology. Heart rate variability: standards of measurement, physiological interpretation, and clinical use. *European Heart J.* **17**, 354-381 (1996).
10. Shaffer, F., McCraty, R. & Zerr, C. A healthy heart is not a metronome: an integrative review of the heart's anatomy and heart rate variability. *Front. Psychol.* **5**(1040), 1-19 (2014).

11. Piskorski, J. & Guzik, P. Asymmetric properties of long-term and total heart rate variability. *Med. Biol. Eng. Comput.* **49**(11), 1289-1297 (2011).
12. Toichi, M., Sugiura, T., Murai, T. & Sengoku A. A new method of assessing cardiac autonomic function and its comparison with spectral analysis and coefficient of variation of R-R interval. *J. Auton. Nerv. Syst.* **62**(1-2), 79-84 (1997).
13. American College of Sports Medicine. General principles of exercise prescription in *ACSM's Guidelines for Exercise Testing and Prescription 10th Edition* (eds. Riebe, D. *et al.*) 152-153 (Wolters Kluwer, Zuid-Holland, 2018).
14. Potter, A. W., Blanchard, L. A., Friedl, K. E., Cadarette, B. S. & Hoyt, R. W. Mathematical prediction of core body temperature from environment, activity, and clothing: the heat strain decision aid (HSDA). *J. Therm. Biol.* **64**, 78-85 (2017).
15. Lin, S.-S. *et al*. Data analytics of a wearable device for heat stroke detection. *Sensors* **18**(12), 4347 (2008).
16. Ciccone, A. B. *et al.* Reminder: RMSSD and SD1 are identical heart rate variability metrics. *Muscle Nerve*. **56**(4), 674-678 (2017).
17. Tulppo, M. P., Mäkikallio, T. H., Seppänen, T., Laukkanen, R.T. & Huikuri, H. V. Vagal modulation of heart rate during exercise: effects of age and physical fitness. *Am. J. Physiol. Heart Circ. Physiol.* **274**(2), H424-H429 (1998).
18. Brennan, M., Palaniswami, M. & Kamen, P. Poincaré plot interpretation using a physiological model of HRV based on a network of oscillators. *Am. J. Physiol. Heart Circ. Physiol.* **283**(5), H1873–H1886 (2002).
19. Pagani, M. *et al.* Power spectral analysis of heart rate and arterial pressure variabilities as a marker of sympatho-vagal interaction in man and conscious dog. *Circ. Res.* **59**(2), 178-193 (1986).
20. Castrillón, C. I. M. *et al.* High-intensity intermittent exercise and autonomic modulation: effects of different volume sessions. *Int. J. Sports Med.* **38**(6), 468-472 (2016).
21. Montano, N. *et al.* Power spectrum analysis of heart rate variability to assess the changes in sympathovagal balance during graded orthostatic tilt. *Circ.* **90**(4), 1826-1831 (1994).
22. Billman, G. E. The LF/HF ratio does not accurately measure cardiac sympatho-vagal balance. *Front. Physiol.* **4**, 26 (2013).
23. Buchheit, M. & Gindre, C. Cardiac parasympathetic regulation: respective associations with cardiorespiratory fitness and training load. *Am. J. Physiol. Heart Circ. Physiol.* **291**(1), H451–H458 (2006).
24. Suzic, L. J. *et al.* Heart rate recovery in elite athletes: the impact of age and exercise capacity. *Clin. Physiol. Funct. Imaging.* **37**(2), 117-123 (2017).
25. Wang, F., Gao, C., Kuklane, K. & Holmér, I. Effects of various protective clothing and thermal environments on heat strain of unacclimated men: the PHS (predicted heat strain) model revisited. *Industrial Health.* **51**, 266-274 (2013).

26. Shaffer F. & Ginsberg, J. P. An overview of heart rate variability metrics and norms. *Front. Public Health* **5**, 258 (2017).
27. Umetani, K., Singer, D. H., McCraty, R. & Atkinson, M. Twenty-four hour time domain heart rate variability and heart rate: relations to age and gender over nine decades. *J. Am. Coll. Cardiol.* **31**(3), 593–601 (1998).
28. Beckers, F., Ramaekers, D. & Aubert, A. E. Approximate entropy of heart rate variability: validation of methods and application in heart failure. *Cardiovasc. Eng.* **1**(4), 177–82 (2001).
29. Pincus, S. M. Approximate entropy as a measure of system complexity. *Proc Natl. Acad. Sci.* **88**(6), 2297-2301 (1991).
30. Richman, J. S. & Moorman, J. R. Physiological time-series analysis using approximate entropy and sample entropy. *Am. J. Physiol. Circ. Physiol.* **278**(6), H2039-H2049 (2000).

Figures

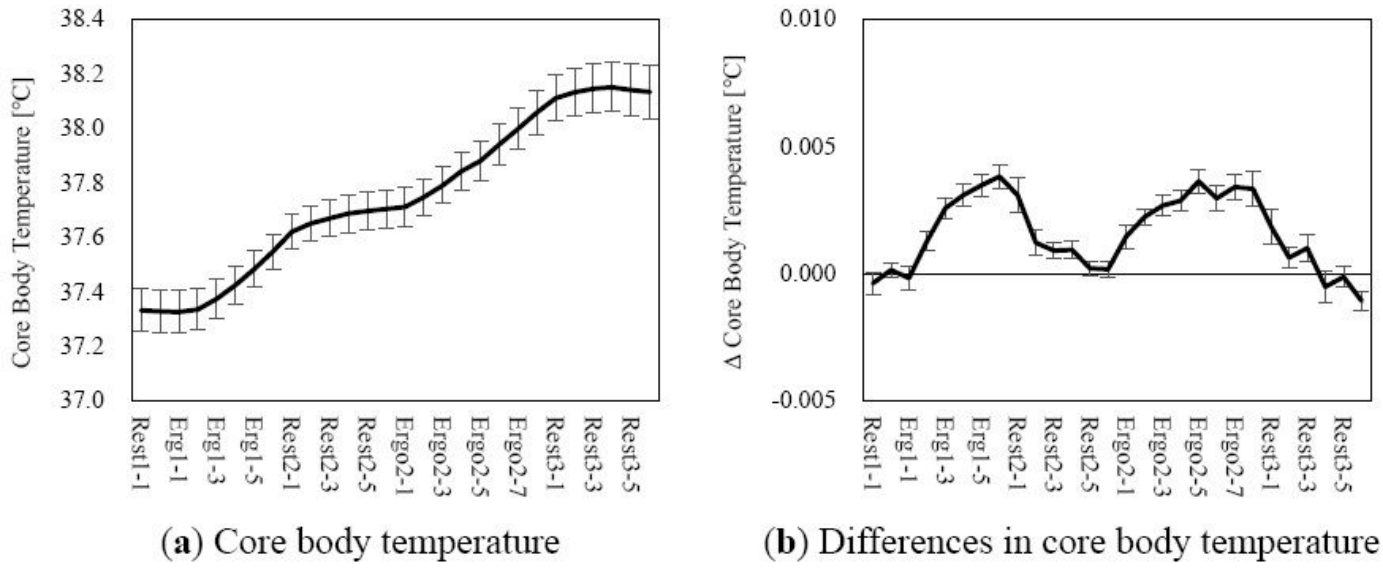

Figure 1

Temporal changes in core body temperature (mean±SE) Note: The core body temperature rose over time, and did not drop, even in the rest block (Rest 2) between exercise blocks. No major differences were observed in the body temperature rise during exercise between the first and second times.

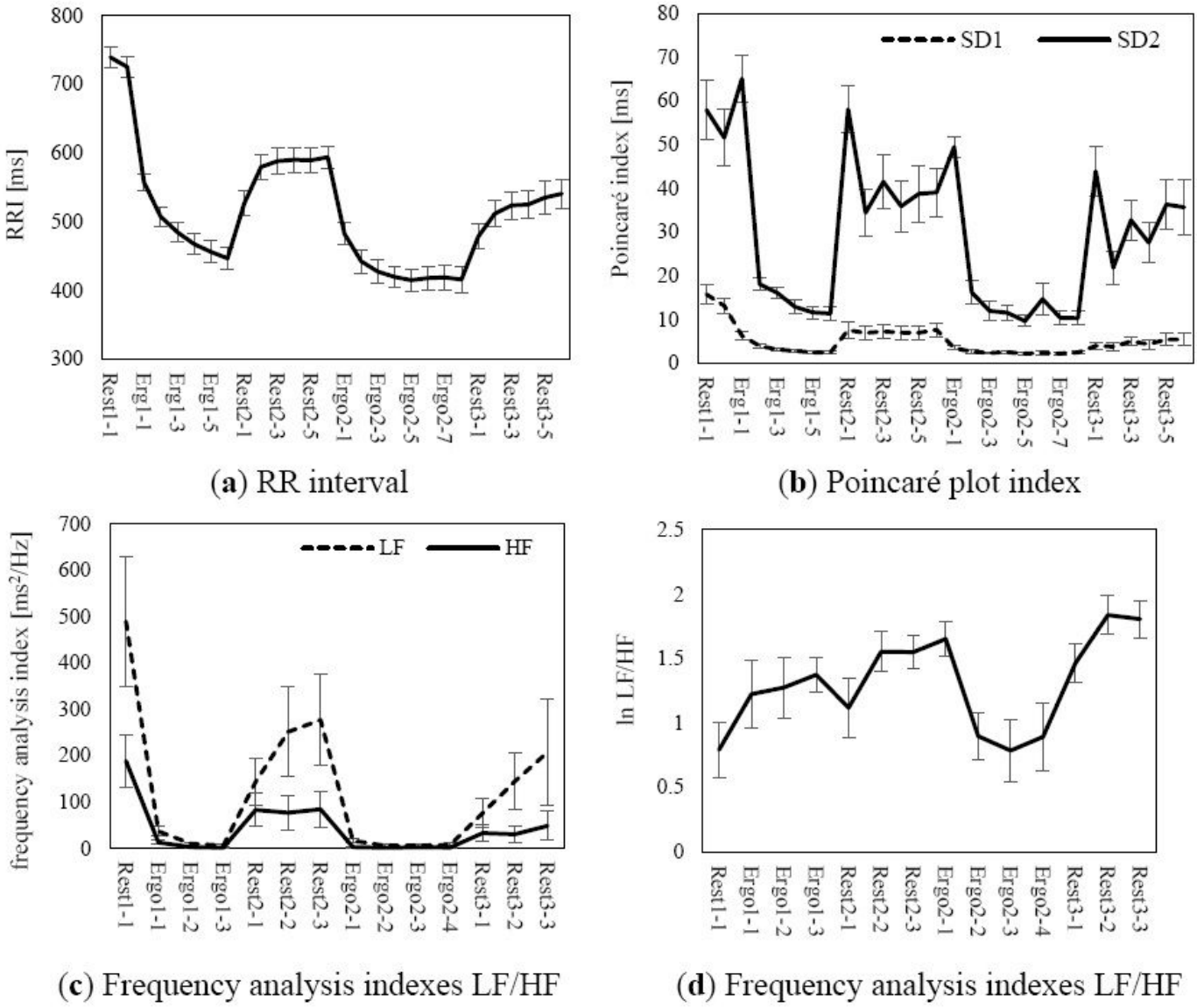

Figure 2

Temporal changes (mean±SE) in ECG indexes Notes: (a) The RRI average dropped rapidly according to the exercise load, and did not return to the pre-exercise state during rest. (b) SD2 exhibited the same trend as RRI. The change in state from the exercise load to resting state was remarkable. (c) (d) The LF and HF components essentially disappeared during exercise loads, and may thus not be suitable for evaluation under those conditions in the stipulated frequency band.

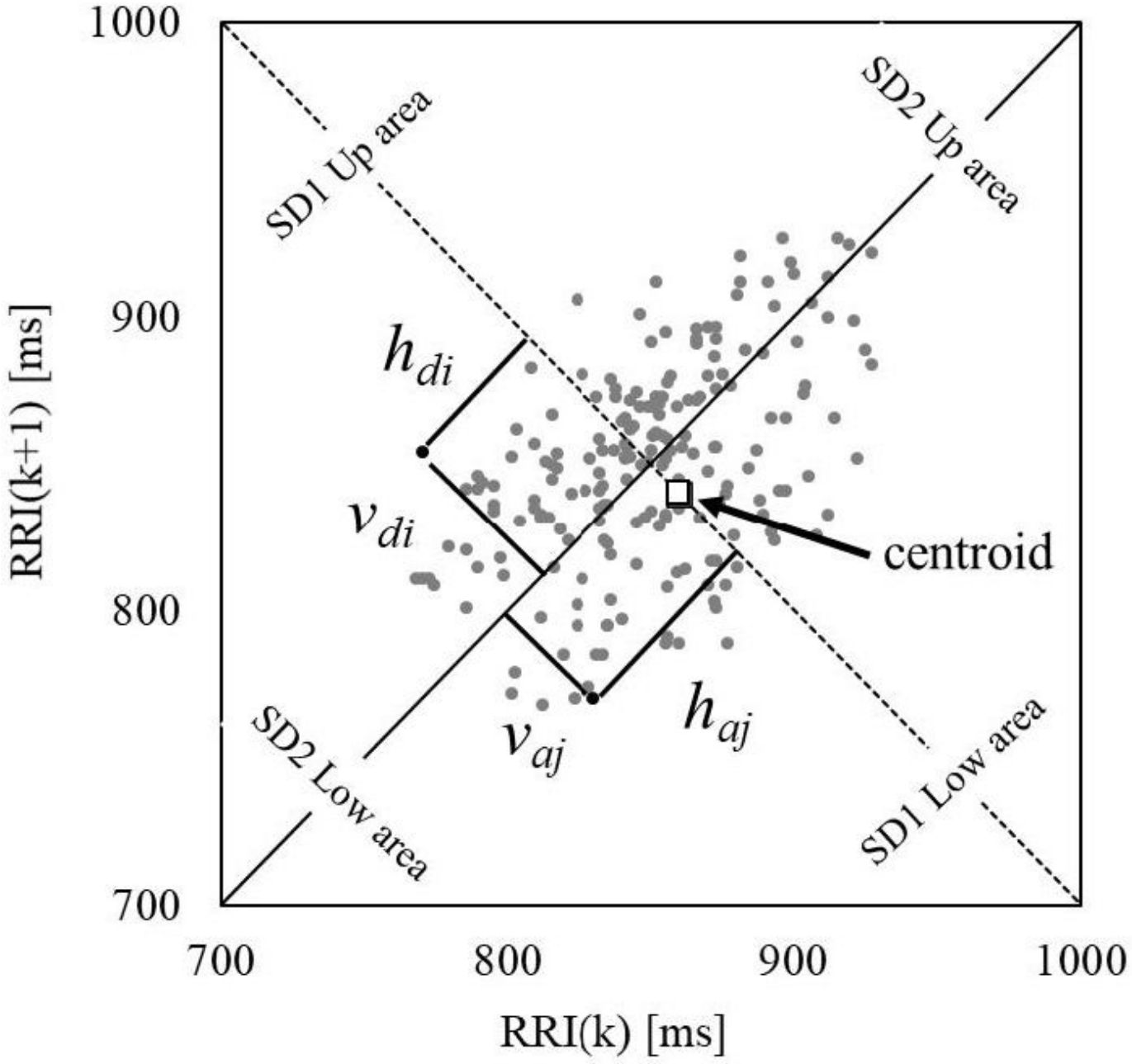

Figure 3

Poincaré plot Note: The Poincaré plot is defined by the lengths of the short side (SD1) and long side (SD2) of an ellipse drawn by RRI(k) and RRI(k+1). In the RRI, SD1 is an index showing rapid change, while SD2 shows subtle change.

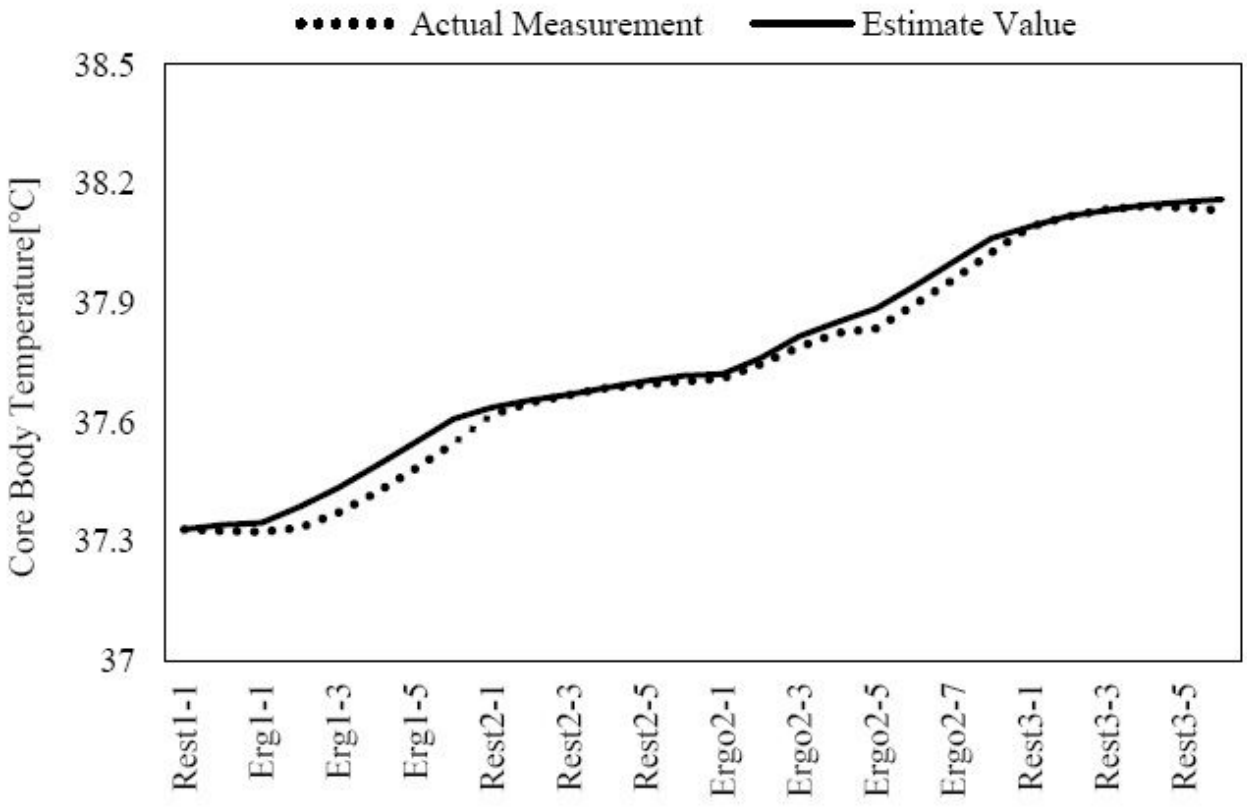

Figure 4

Actual measurements and estimates of core body temperature (average of all test runs) Note: The dotted line shows actual measured values, while the solid line shows estimated values. The mean error was -0.007°C, while the mean error rate was -0.02%. See Supplementary Fig. 1 for actual measurements and estimates from all 16 test runs.

Supplementary Files

This is a list of supplementary files associated with this preprint. Click to download.

- SupplementaryFigure.pdf